



# Electronic Topological Transitions in CuNiMnAl and CuNiMnSn under pressure from first principles study

P. Rambabu <sup>a, b</sup>, V. Kanchana <sup>a, \*</sup>

<sup>a</sup> Department of Physics, Indian Institute of Technology Hyderabad, Kandi, Sangareddy 502 285, Telangana, India

<sup>b</sup> Department of Pure and Applied Physics, Guru Ghasidas Vishwavidyalaya, Koni, Bilaspur 495 009, Chhattisgarh, India

## ARTICLE INFO

### Article history:

Received 29 January 2018

Received in revised form

15 March 2018

Accepted 30 March 2018

Available online 4 April 2018

### Keywords:

Electronic Topological Transitions (ETTs)

Fermi surface (FS) topology

Quaternary full Heusler alloys

## ABSTRACT

A detailed study on quaternary ordered full Heusler alloys CuNiMnAl and CuNiMnSn at ambient and under different compressions is presented using first principles electronic structure calculations. Both the compounds are found to possess ferromagnetic nature at ambient with magnetic moment of Mn being  $3.14 \mu_B$  and  $3.35 \mu_B$  respectively in CuNiMnAl and CuNiMnSn. The total magnetic moment for both the compounds is found to decrease under compression. Fermi surface (FS) topology change is observed in both compounds under pressure at  $V/V_0 = 0.90$ , further leading to Electronic Topological Transitions (ETTs) and is evidenced by the anomalies visualized in density of states and elastic constants under compression.

© 2018 Elsevier Masson SAS. All rights reserved.

## 1. Introduction

Ever since the discovery of Heusler compounds, a continuous growing interest is observed among researchers because of their applications in spintronics [1–4], data storage, spin valves [5], magnetic tunnel junctions [6–8], optoelectronics [9], superconductivity [10–12], shape memory alloys [13] and thermoelectrics [14–16] etc. These Heusler compounds are ternary inter-metallic compounds, having two transition metals and one main group element. These compounds can be divided into two groups: namely ternary and quaternary alloys. The ternary Heusler alloys again can be classified into two families, full ternary  $X_2YZ$  and half ternary  $XYZ$  ( $X$  and  $Y$  are transition-metal elements,  $Z$  is sp element) alloys. The quaternary Heusler alloys have general formula  $XX'YZ$  which is generated by substituting one of the two  $X$  atoms in full ternary Heusler alloys  $X_2YZ$  by a different transition metal  $X'$  [17] atom.

Since both the compounds CuNiMnAl and CuNiMnSn under study are metals [18], it is very important to understand their Fermi surface characteristics at ambient as well as under compression and their corresponding Electronic Topological Transitions (ETT), if any. The Fermi surface (FS) of a metal is an important tool to understand various properties of a metallic material such as structural transition, elastic, magnetic properties etc. The geometrical

characteristics of Fermi surface, such as the shape, curvature, and cross-sectional area are related to the physical properties of metals. In general, the ETTs are very well explained by Fermi surface topology. The connectivity of the Fermi surfaces can change at some particular points due to the variation of thermal, static or chemical pressure, due to which there would be an anomalous behavior in thermodynamic, elastic and transport properties, which was pointed out first time by Lifshitz [19]. The change in FS connectivity is may be due to opening up or closing of electron or hole pockets, or due to the formation or pinching off of a neck [20] and one of these changes leads to ETTs. The ETTs could be achieved by changing the electron per atom ratio, by alloying, or by applying pressure or uniaxial stress [21]. In magnetic hcp-Co [22], the authors studied Fermi surface topology under pressure and observed hcp-Co to become non-magnetic at 180 GPa with a series of ETTs under different pressures. Especially at 80 GPa, there is a transition which results in a large increase in DOS at Fermi level and it is the reason for the anomalies in various elastic properties at that pressure. Recently, in antiferromagnetic  $Zr_2TiAl$  [23] the authors also observed three ETTs at  $V/V_0 = 0.96, 0.92$  and  $0.85$ , due to which a sudden drop in the magnetic moment of Ti atom is observed under compression and they also observed a magnetic to non-magnetic phase transition under compression due to the disappearance of the Ti magnetic moment, which tends to zero at  $V/V_0 = 0.75$  (46 GPa). In non-magnetic Nb-based [24] A-15 compounds  $Nb_3X$  ( $X = Al, Ga, In, Ge, \text{ and } Sn$ ), the authors predicted ETTs at different compressions in all the compounds.

\* Corresponding author.

E-mail address: [kanchana@iith.ac.in](mailto:kanchana@iith.ac.in) (V. Kanchana).

The Ni-Mn based high entropy Heusler alloys have been extensively investigated in search of efficient magnetic refrigerant materials because of their high magnetic entropy change, wide operating temperature window, low hysteresis loss and high mechanical stability [25]. Equiatomic compositions maximize the configurational entropy of random solid solutions [26] and both compounds in the present study are equiatomic in nature. The high entropy quaternary full Heusler alloys CuNiMnAl and CuNiMnSn, prepared by Aron-Dine et al. [18], are found to exhibit LiMgPdSn-type  $L2_1$  structure and are ferromagnetic in nature. However, to the best of our knowledge, no details regarding electronic structure, magnetic nature, Fermi surface topology and mechanical stability are available till now for these compounds at ambient and under pressure. Our main goal in this paper is to investigate elastic, Fermi surface topology of both the compounds at ground state as well as under compression using first principles approach. Though no phase transition from magnetic to non-magnetic phase is observed in both compounds, ETTs are clearly seen from Fermi surface studies under compression.

## 2. Computational details

Self consistent FP-LAPW spin polarized calculations as implemented in WIEN2K [27] package were carried out on both CuNiMnAl and CuNiMnSn compounds to solve the Kohn-Sham equations. The PBE-GGA [28] (Perdew-Burke-Ernzerhof parametrization of the generalized gradient approximation) was used for the exchange correlation potential. The matrix size (convergence) is determined by  $R_{MT} * K_{max}$  and it was set to 7 and  $G_{max}$  was set to a value of 12 here. The muffin-tin sphere radii used in the calculations for Cu, Ni, Mn, Al and Sn respectively were 2.15 a.u., 2.1 a.u., 2.0 a.u., 1.95 a.u. and 2.25 a.u. The convergence criteria for energy was set as  $10^{-5}$  Ry. The special k-points in the Irreducible Brillouin Zone (IBZ) were 4000 according to Monkhorst-Pack scheme [29]. Tetrahedron method [30] was used to integrate the Brillouin zone. All Fermi surface calculations were done with  $44 \times 44 \times 44$  k-mesh in order to get smoother Fermi surfaces. The equilibrium lattice constant for the studied compounds was obtained using Birch-Murnaghan [31] equation of state to fit the total energies as a function of primitive cell volume. The elastic constants were calculated using the method [32] provided by Morteza Jamal et al. as implemented in Wien2K.

## 3. Results and discussions

### 3.1. Ground state and magnetic properties

The compounds CuNiMnAl and CuNiMnSn, are found to have space group  $F\bar{4}3m$  (No. 216) with atomic positions of Cu, Ni, Mn and Al/Sn at A (0, 0, 0), B (1/2, 1/2, 1/2), C (1/4, 1/4, 1/4) and D (3/4, 3/4, 3/4) respectively. To confirm the ground state of the investigated compounds, we have optimized the compounds in non-magnetic (NM), ferromagnetic (FM) and ferrimagnetic (FRM) cases and the optimized curves are plotted in Fig. 1. The optimized lattice parameters are given in Table 1 for both the compounds along with experimental and other theory values and found that our results are in acceptable range. It can be seen that at low volume (high pressure), the energy difference between FM and NM curves decreases for both the compounds implying the reduced magnetic moment with increasing compression (pressure). The energy difference  $\Delta E$  between FM and FRM states is 0.042 Ry for CuNiMnAl and for CuNiMnSn case the difference surprisingly becomes 0.0 Ry indicating that both FM and FRM states are competing with each other in this compound. From the optimized plots, it is confirmed that CuNiMnAl is found to have ferromagnetic ground state. Though the FM and FRM states are competing with each other in CuNiMnSn, from the observed magnetic moments, it is expected that CuNiMnSn might possess a stable ferromagnetic ground state. The calculated total magnetic moment of the present compounds is found to be 3.626 and 3.811  $\mu_B$  for CuNiMnAl and CuNiMnSn respectively, indicating these compounds to possess almost similar magnetic properties. The calculated magnetic moments for individual atoms for both the compounds are shown in Table 2.

The calculated band structure and Fermi surface (FS) plots at ambient (at  $V/V_0 = 1.00$ ) in both majority and minority spin cases are given in Fig. 2 for CuNiMnAl and in Fig. 3 for CuNiMnSn. From the overall observation of band structure, majority spin bands are found to be almost similar in both the compounds and minority spins also follow the same similarity. In CuNiMnAl, three bands are

**Table 1**

Calculated lattice parameters given in  $\text{\AA}$  along with experimental and theoretical data.

Compounds	Expt	Theoretical	Present work
CuNiMnAl	5.89 [18]	5.86 [18]	5.84
CuNiMnSn	6.08 [18]	6.02 [18]	6.12

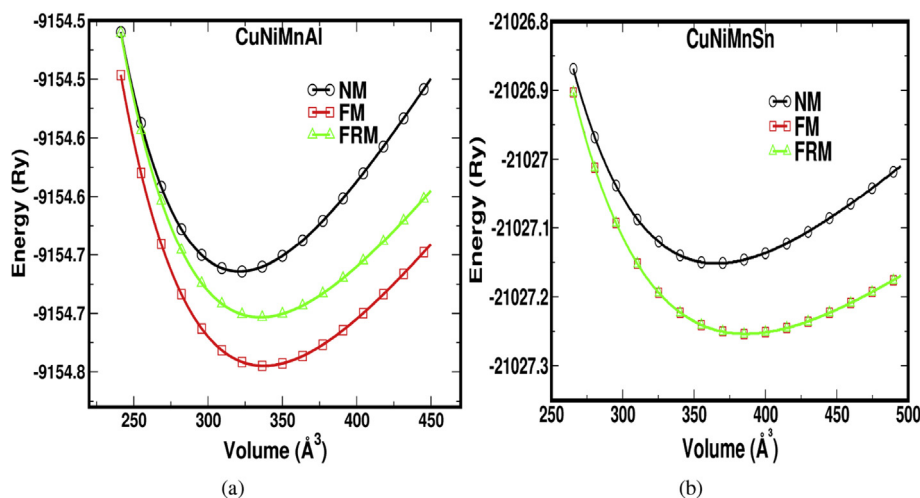


**Fig. 1.** Calculated total energy versus volume for nonmagnetic (NM), ferromagnetic (FM) and ferrimagnetic (FRM) states for (a) CuNiMnAl and (b) CuNiMnSn compounds.

**Table 2**  
Magnetic moments of individual atoms for CuNiMnAl and CuNiMnSn in ferromagnetic (FM) and ferrimagnetic (FRM) configurations. Magnetic moments are given in Bohr magneton ( $\mu_B$ ).

		Cu	Ni	Mn	Al/Sn	Interstitial	Total/cell
CuNiMnAl	FM	0.04906	0.33866	3.14273	-0.03700	0.13250	3.62594
	FRM	0.04910	0.33868	3.14295	-0.03700	0.13235	3.62609
CuNiMnSn	FM	0.02284	0.23761	3.35132	-0.03084	0.23048	3.81142
	FRM	0.02290	0.23766	3.35129	-0.03081	0.23040	3.81145

found to cross the Fermi level ( $E_F$ ) in both the spin cases and correspondingly we have three FS's for each spin and are given in Fig. 2. In majority spin case of CuNiMnAl (from Fig. 2 (a)), first band is found to cross from valence band to conduction band at  $\Gamma$  resulting in a hole natured spherical FS at the same point as shown in Fig. 2 (c). Remaining two bands in majority spin are found to cross from conduction band to valence band and have electron nature as shown in Fig. 2 (d and e). In the minority spin case of CuNiMnAl (from Fig. 2 (b)), we found two bands to cross  $E_F$  at L point from valence to conduction band indicating hole nature and the other remaining band is found to cross  $E_F$  at X point from conduction band to valence band indicating electron nature as shown in Fig. 2 (f, g, h). These bands at X and L have states

contributed from Ni- $d_{e_g}$  and Mn -  $d_{t_{2g}}$  respectively. In the case of CuNiMnSn (Fig. 3), the majority spin band structure and FS scenario is same as CuNiMnAl majority spin but in minority spin case, we have only one band to cross the  $E_F$  at X point and the corresponding FS is shown in Fig. 3 (f). This band is attributed to Ni- $d_{e_g}$  contribution. The Brillouin Zone with high symmetry points for both compounds is shown in Fig. 3 (g).

To explore further, we have calculated total and atom projected density of states (DOS) for both the compounds at  $V/V_0 = 1.00$  and are plotted in Fig. 4. The DOS of majority spin channel for CuNiMnAl near  $E_F$  is mainly contributed by Mn- $d_{t_{2g}}$  and Ni- $d_{t_{2g}}$  orbitals and the DOS of minority spin channel for CuNiMnAl near  $E_F$  has similar contribution which can be seen from Fig. 4 (a). From Fig. 4 (a), it can

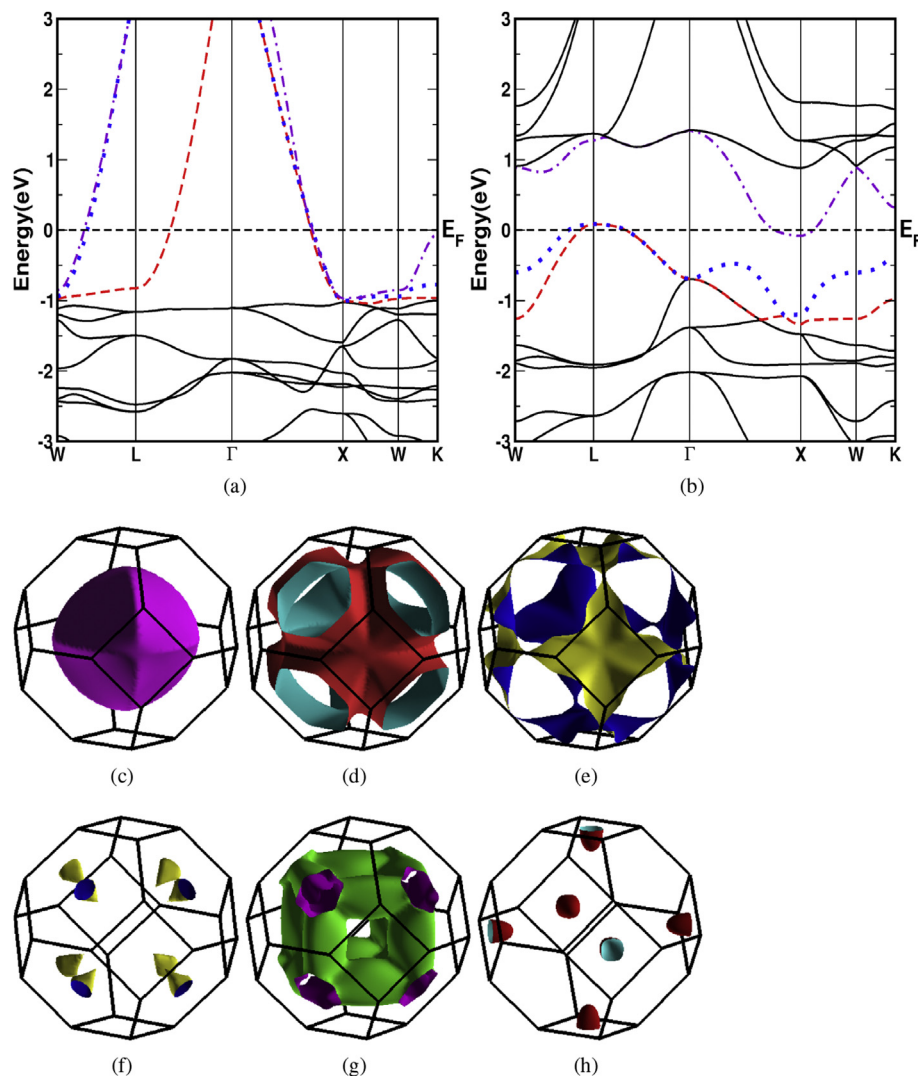


**Fig. 2.** Band structure of CuNiMnAl (a) majority spin and (b) minority spin case at  $V/V_0 = 1.00$  and their Fermi surface in majority spin (c, d, e) and minority spin (f, g, h) cases.

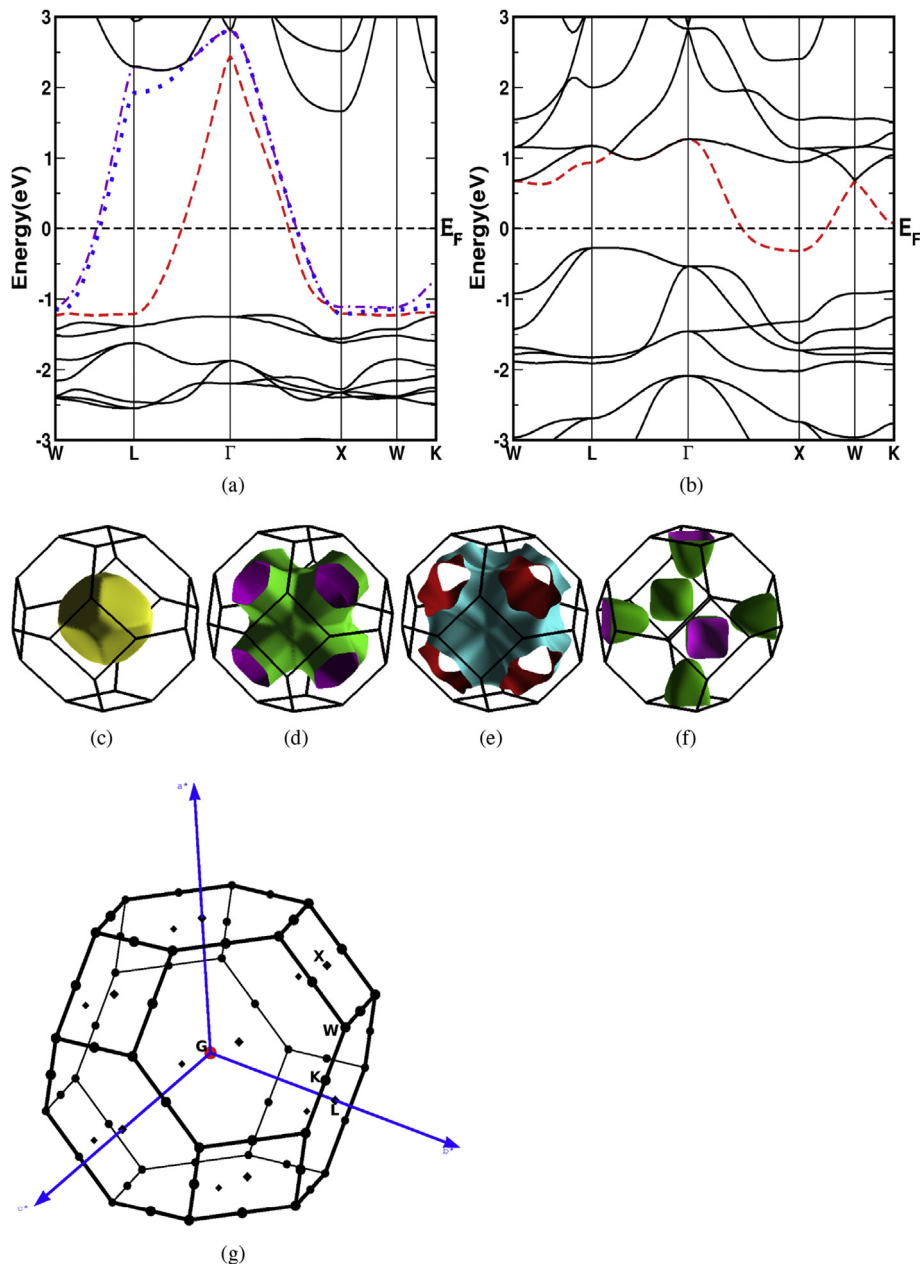


**Fig. 3.** Band structure of CuNiMnSn (a) majority spin and (b) minority spin case at  $V/V_0 = 1.00$  and their Fermi surface in majority spin (c, d, e) and minority spin (f) cases. The Brillouin Zone with High symmetry points is given in (g).

be seen that the bonding between Mn and Ni atoms may be stronger indicating that the Heisenberg's exchange coupling strength may be stronger between them which is to be confirmed. For CuNiMnSn, the DOS of majority spin channel near  $E_F$  is mainly contributed by Ni- $d_{t_{2g}}$  and Mn- $d_{t_{2g}}$  orbitals and for minority spin channel, the DOS near  $E_F$  is mainly contributed by Mn- $d_{e_g}$  and Ni- $d_{e_g}$  orbitals as shown in Fig. 4 (b). From Fig. 4 (b), it is clear that the interaction between Mn and Ni atoms is not as stronger as in the case of CuNiMnAl compound and hence its Mn-Ni exchange strength may be weaker compared to CuNiMnAl, and Mn-Mn interaction may be dominating which need to be verified from exchange interaction calculations. The contribution from  $s$  and  $p$ -orbitals near  $E_F$  is almost negligible for both the compounds and hence they are not shown in the graphs.

To understand the charge flow, Bader charge analysis for the

constituent atoms is done at ambient and under compression for both compounds. The Pauling electro negativity values for Cu, Ni, Mn, Al and Sn are 1.90, 1.91, 1.55, 1.61 and 1.96 respectively. Since the elements with higher electro negativity attract the charge from lower ones, there is a possibility of charge transfer from (Mn, Al) to (Cu, Ni) in CuNiMnAl which can be clearly seen from Table 3. Also, there is a possibility of charge transfer from Mn to (Cu, Ni) in CuNiMnSn which can be seen from Table 3. The Bader charge on Mn and Al respectively are 0.39e and 1.51e which lose charge and are accepted by Cu and Ni which are having Bader charge of -0.83e and -1.07e respectively at  $V/V_0 = 1.00$  in CuNiMnAl compound. Also for CuNiMnSn, the Bader charge for Mn and Sn are 0.45e and 0.30e respectively which lose their charge and this charge is accepted by Cu and Ni which have Bader charge of -0.28e and -0.48e respectively at  $V/V_0 = 1.00$ .

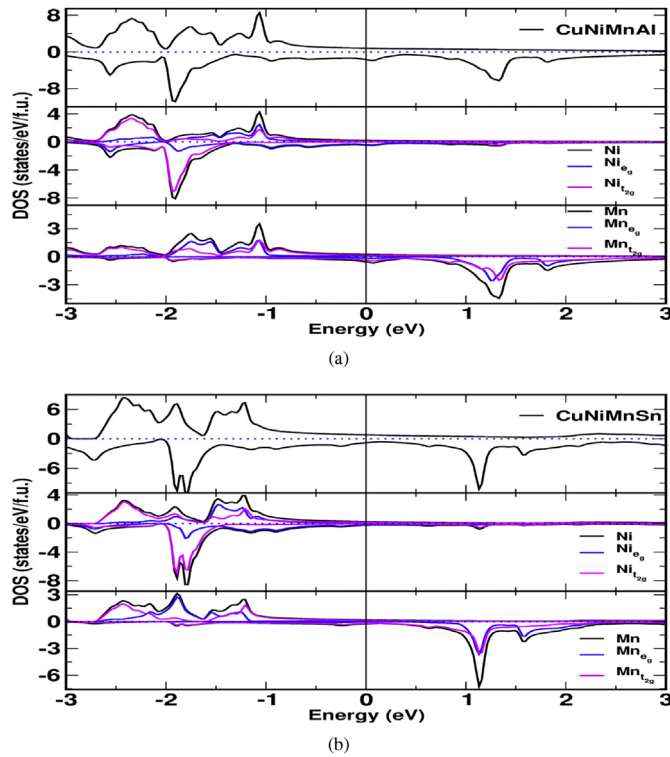


Fig. 4. Density of States of (a) CuNiMnAl and (b) CuNiMnSn compounds.

Table 3

Calculated Bader charge analysis for CuNiMnAl and CuNiMnSn for different  $V/V_0$  ratios. The charge is in the units of electronic charge  $e$ .

$V/V_0$	CuNiMnAl				CuNiMnSn			
	Cu	Ni	Mn	Al	Cu	Ni	Mn	Sn
1.00	-0.83	-1.07	0.39	1.51	-0.28	-0.48	0.45	0.30
0.95	-0.89	-1.15	0.37	1.67	-0.29	-0.49	0.44	0.34
0.90	-0.94	-1.21	0.34	1.81	-0.29	-0.51	0.42	0.39
0.85	-0.98	-1.27	0.31	1.95	-0.30	-0.52	0.40	0.43
0.80	-1.01	-1.32	0.26	2.07	-0.30	-0.54	0.38	0.46

### 3.2. Elastic properties

In order to ensure the mechanical stability, the elastic constants  $C_{ij}$  of all the investigated compounds are calculated from which, one can check the phase stability of the compounds and they also provide an estimation of the strength and indirectly their melting temperature. To the best of our knowledge, no information is available on elastic constants for these compounds till now either experimentally or theoretically and these results serve as prediction for future studies. All the compounds in the present case are in cubic phase and have three non-zero elastic constants  $C_{11}$ ,  $C_{12}$  and  $C_{44}$  respectively. The calculated elastic constants at  $V/V_0 = 1.00$  for both compounds satisfy the Born mechanical stability criteria [33] i.e.  $C_{11} > 0$ ,  $C_{44} > 0$ ,  $C_{11} > C_{12}$  and  $C_{11} + 2C_{12} > 0$ , indicating all the compounds to be mechanically stable. The elastic properties such as Young's modulus ( $E$ ), average shear modulus ( $G$ ), Poisson's ratio ( $\sigma$ ) and anisotropy factor ( $A$ ) etc. are determined from Voigt-Reuss-Hill approximation [34]. The relation between elastic moduli  $C_{11}$ ,  $C_{12}$  and  $C_{44}$  and the other parameters are found elsewhere [35–37].

Since the average shear modulus ( $G$ ) is a measure of resistance to reversible deformations upon shear stress and represents the resistance to plastic deformation, the hardness of the material can

be determined more accurately from  $G$ . The value of  $G$  is 52.55 GPa for CuNiMnAl and 34.3 GPa for CuNiMnSn. The compounds are found to be anisotropic since the anisotropy factor  $A$  is different from unity. The Young's modulus  $E$  values are 140.19 and 94.67 GPa for CuNiMnAl and CuNiMnSn respectively and indicate these materials to be stiffer. The ratio of lateral to longitudinal strain in uniaxial tensile stress is known as Poisson's ratio [38] ' $\sigma$ ', which is a measure of compressibility. The typical range of  $\sigma$  is 0.2–0.49 and is around 0.3 for most of the materials. The Poisson's ratio ' $\sigma$ ' for both the compounds varies in the range of 0.33–0.39. Further, Poisson's ratio also provides information about the characteristics of the bonding forces. For central forces in solids,  $\sigma$  lies within the range 0.25–0.5. Since  $\sigma$  for both compounds lies in this limit, it demonstrates that the inter-atomic forces in these compounds are central forces. Since bulk modulus  $B$  represents the resistance to fracture, while the shear modulus  $G$  represents the resistance to plastic deformation, the Pugh's index of ductility [39]  $\frac{B}{G}$  will give the information of whether the material is ductile or brittle in nature depending on the critical value 1.75. Present compounds are found to be ductile in nature from the calculated Pugh's values. Also, if the Poisson's ratio ' $\sigma$ ' is greater than 0.26, then the material is ductile, otherwise it is brittle in nature. For both the compounds  $\sigma$  is greater than 0.26 which is another indication that these materials are ductile in nature. Another parameter which indicates the ductility is Cauchy's pressure  $P_c$ , which is positive for both the compounds demonstrating the present compounds to be ductile in nature. All the elastic properties for both compounds at  $V/V_0 = 1.00$  are given in Table 4. The Debye temperature is also an important parameter which is closely related to many physical properties of a solid. It actually distinguishes between high and low temperature regions of a solid and can be directly determined from the mean sound velocity. The Calculated Debye temperature values for both compounds at  $V/V_0 = 1.00$  are also given in the same Table 4.

### 4. Pressure effect

Effect of pressure is always an interesting phenomenon for a physicist. In the present compounds also, we are interested to study the behavior of the compounds under pressure. Here we have applied uniform pressure up to  $V/V_0 = 0.80$  with step size of  $V/V_0 = 0.05$ . The calculated total magnetic moment is found to decrease with applied uniform compression. The variation of magnetic moment with  $V/V_0$  for both the compounds is studied and the results are presented in Fig. 5. From Fig. 5, it is clear that the total magnetic moment/cell is found to decrease under compression for both the compounds. The reason for this may be due to the

Table 4

Elastic properties of CuNiMnAl and CuNiMnSn at  $V/V_0 = 1.00$ .

Parameter	CuNiMnAl	CuNiMnSn
$C_{11}$ (GPa)	160.28	137.36
$C_{12}$ (GPa)	130.93	128.47
$C_{44}$ (GPa)	114.11	94.08
$A$	7.77	21.15
$G_V$ (GPa)	74.34	58.22
$G_R$ (GPa)	30.76	10.38
$B$ (GPa)	140.71	131.43
$G$ (GPa)	52.55	34.30
$E$ (GPa)	140.19	94.67
$B/G$	2.68	3.83
$\sigma$	0.33	0.38
$P_c = C_{11} - C_{12}$	29.35	8.89
$V_l$ (km/s)	11.15	9.08
$V_t$ (km/s)	5.57	3.99
$V_m$ (km/s)	6.25	4.51
$\theta_D$ (K)	505.03	348.75

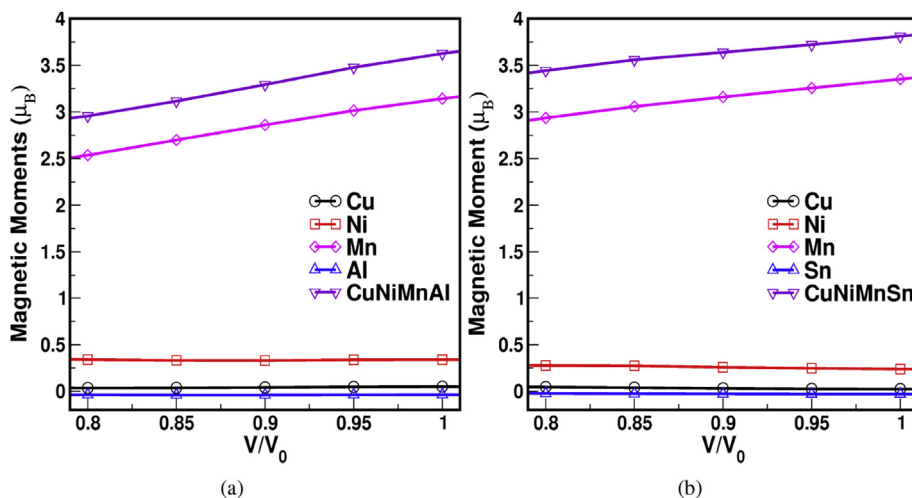


Fig. 5. Variation of Magnetic moment of (a) CuNiMnAl and (b) CuNiMnSn compounds with  $V/V_0$  ratio.

broadening of Mn 3d-band and the non-sustainability for magnetic polarization.

The change of Fermi surface topology under compression is studied in majority and minority spin cases and is presented in Fig. 6 and Fig. 7 respectively for both CuNiMnAl and CuNiMnSn compounds. For CuNiMnAl under compression, the number of bands that cross Fermi level in majority spin case do not change while in minority spin case they are found to decrease from three to one as  $V/V_0$  goes from 1.00 to 0.90. The corresponding FS topology is shown in Fig. 6 in which the FS topology almost does not change in majority spin case while it changes in minority spin case and the changes can be seen for  $V/V_0 = 0.90$ , where one can find only one FS, since only one band crosses Fermi level at this compression for CuNiMnAl. This is more clear from the band structure and its corresponding FS topology for  $V/V_0 = 0.90$  case in minority spin case of CuNiMnAl as presented in Fig. 8. Since the number of bands (or its corresponding FSs) that cross the Fermi level drop from three to one as  $V/V_0$  changes from 1.00 to 0.90 in minority case of

CuNiMnAl, one can say that there is an Electronic Topological Transition (ETT) at  $V/V_0 = 0.90$ . Further, as  $V/V_0$  goes down, the size of the electron wave packet increases which can be seen for  $V/V_0 = 0.85, 0.80$  cases from Fig. 6. For CuNiMnSn under compression, the number bands that cross Fermi level is three in majority spin case and they don't change with compression which is reflected from Fig. 7, while only one band is found to cross at X point in minority spin case and its corresponding FS can be seen from Fig. 7. As  $V/V_0$  changes from 1.00 to 0.90, we find another band to cross at K point in minority spin case at  $V/V_0 = 0.90$  and its FS can be seen in Fig. 7. The arrow in Fig. 7 points out the evolution of electron wave packet at K-point at  $V/V_0 = 0.90$ . This is more clear from the band structure and its corresponding FS topology for  $V/V_0 = 0.90$  case in minority spin case of CuNiMnSn as presented in Fig. 9. Since the number of bands (or its corresponding FSs) that cross Fermi level increase from one to two as  $V/V_0$  goes from 1.00 to 0.90 in minority case of CuNiMnSn, an ETT is reported at  $V/V_0 = 0.90$  as the opening up or closing of the electron or hole packets under uniaxial stress

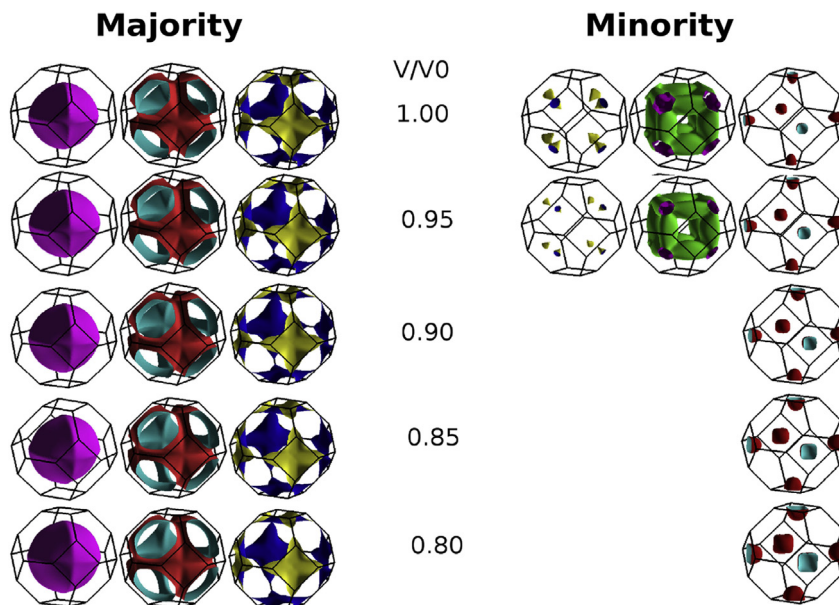


Fig. 6. Fermi surface of CuNiMnAl at different  $V/V_0$  ratios for majority and minority spin cases.

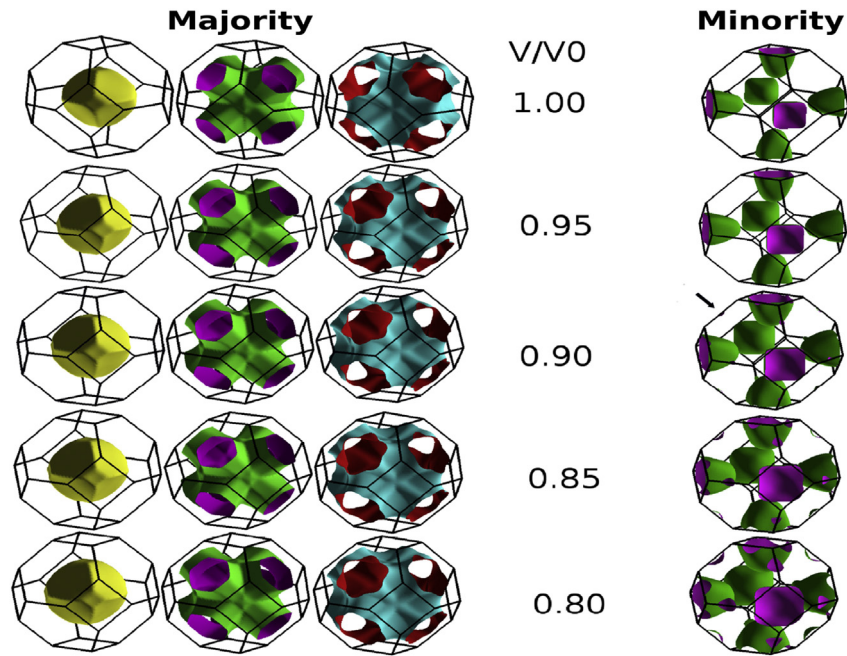


Fig. 7. Fermi surface of CuNiMnSn at different  $V/V_0$  ratios for majority and minority spin cases.

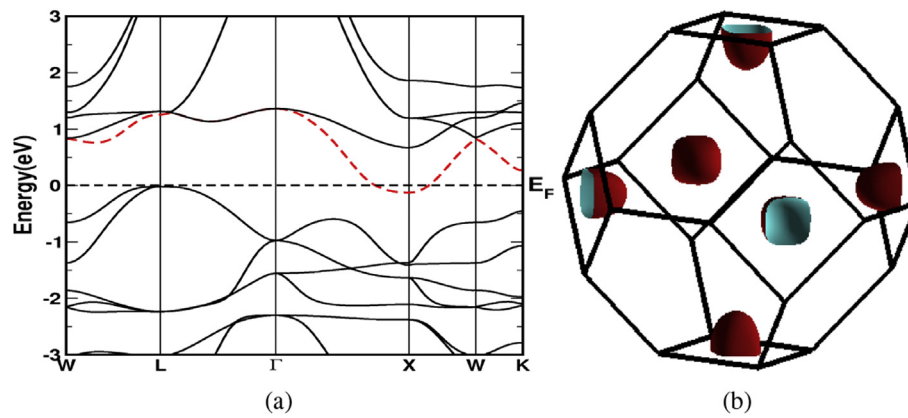


Fig. 8. (a) Band structure and (b) its corresponding Fermi surface of CuNiMnAl at  $V/V_0 = 0.90$ .

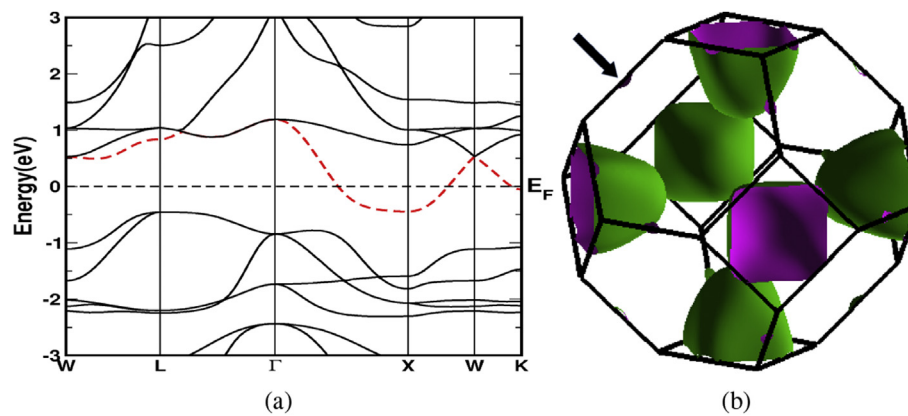
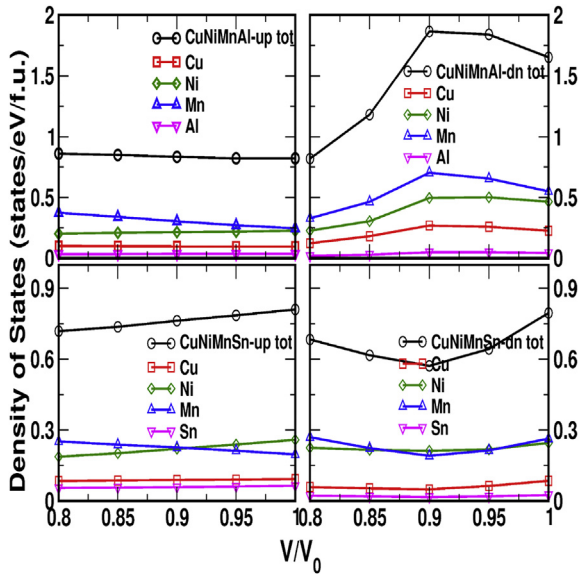


Fig. 9. (a) Band structure and (b) its corresponding Fermi surface of CuNiMnSn at  $V/V_0 = 0.90$ . The arrow indicates the evolution of additional electron pocket at K-point.



**Fig. 10.** Variation of Density of States of CuNiMnAl and CuNiMnSn compounds at Fermi level  $E_F$  with  $V/V_0$  ratio in both majority and minority spin cases.

leads to ETTs. Again if  $V/V_0$  is further reduced, the size of the two electron wave packets at X and K points increases as can be seen in Fig. 7.

To know the effect of pressure on the density of states at Fermi level, we have calculated the total and atom projected DOS under compression for both the compounds and are presented in Fig. 10. From this, the DOS varies monotonically in majority spin case where as there is a non-monotonic variation in down-spin case in both the compounds. This non-monotonic behavior is observed in both compounds in minority spin cases at  $V/V_0 = 0.90$ , where we have observed the changes in the band and FS topology in both the compounds which also supports the idea of ETT at  $V/V_0 = 0.90$  for both compounds.

The Bader charges of all the constituent elements for both compounds at different  $V/V_0$  ratios are shown in Table 3. As  $V/V_0$  decreases, there is a continuous flow of charge from Mn to Ni in CuNiMnAl compound and (Mn, Sn) loose more charge and may be gained by Ni in CuNiMnSn compound as can be seen from Table 3.

To check the mechanically stable nature in the present compounds, we have calculated the single crystalline elastic constants under compression and are plotted in Fig. 11. It is observed that the compounds are found to be mechanically stable up to the

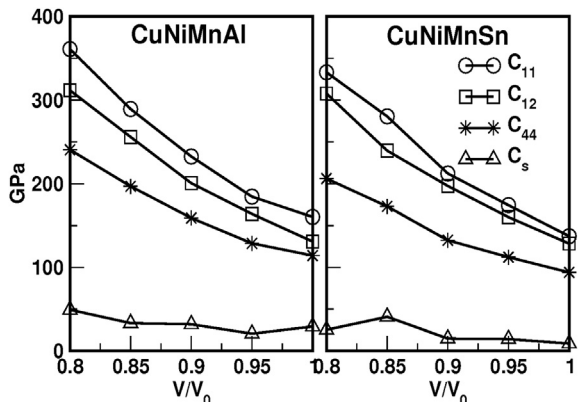


**Fig. 11.** Variation of elastic constants  $C_{ij}$  and shear modulus  $C_s$ .

compression studied. It is also observed that, the elastic constants  $C_{ij}$  are found to increase under compression for both the compounds, together with a softening in  $C_{44}$  around  $V/V_0 = 0.90$  in both the compounds. In earlier reports, the authors [23] quoted in their paper that the non linear behavior in the elastic shear modulus  $C_s = (C_{11} - C_{12})/2$  leads to ETTs and the anomalies present in  $C_s$  [40] also lead to ETTs. Hence from the calculated value of  $C_s$  for both CuNiMnAl and CuNiMnSn, one can find a non linear behavior under compression in both the compounds especially at  $V/V_0 = 0.90$ , again indicating the ETT at that particular  $V/V_0$  value in both compounds.

## 5. Conclusions

The high entropy quaternary Heusler alloys CuNiMnAl and CuNiMnSn are studied under compression theoretically through DFT and are found to be ferromagnetic. The magnetic moment/cell is found to decrease for both compounds under compression. The mechanical stability of these compounds is confirmed through elastic properties. The pressure effect on both compounds upto  $V/V_0 = 0.80$  is studied and the presence of Electronic Topological Transitions (ETTs) at  $V/V_0 = 0.90$  in both the compounds is evidenced through FS topology.

## Acknowledgement

The authors P.R and V.K would like to acknowledge IIT-Hyderabad for providing computational facility. P.R acknowledges Guru Ghasidas Vishwavidyalaya, Bilaspur, Chhattisgarh for sponsoring his Ph.D programme. Also P.R acknowledges P.V. Sreenivasa Reddy and Sreeparvathy P.C for their timely help and fruitful discussions.

## References

- [1] I. Galanakis, K. Özdoğan, E. Şaşıoğlu, B. Aktaş, Phys. Rev. B 75 (2007) 092407.
- [2] L. Zhang, Z.X. Cheng, X.T. Wang, R. Khenata, H. Rozale, J. Supercond. Nov. Magnetism (2017). <https://doi.org/10.1007/s10948-017-4182-6>.
- [3] Peng-Li Yan, Jian-Min Zhang, Bo Zhou, Ke-Wei Xu, J. Phys. D Appl. Phys. 49 (2016) 255002.
- [4] Benjamin Balke, Sabine Wurmehl, Gerhard H. Fecher, Claudia Felser, Jürgen Kübler, Sci. Technol. Adv. Mater. 9 (2008) 014102.
- [5] Koichiro Inomata, Susumu Okamura, Ryota Goto, Nobuki Tezuka, Jpn. J. Appl. Phys. 42 (2003). Pt. 2, No. 4B.
- [6] Y. Sakuraba, M. Hattori, M. Oogane, Y. Ando, H. Kato, A. Sakuma, T. Miyazaki, Appl. Phys. Lett. 88 (2006) 192508.
- [7] N. Tezuka, N. Ikeda, F. Mitsuhashi, S. Sugimoto, Appl. Phys. Lett. 94 (2009) 162504.
- [8] Sumito Tsunegi, Yuya Sakuraba, Mikihiko Oogane, Koki Takanashi, Yasuo Ando, Appl. Phys. Lett. 93 (2008) 112506.
- [9] Vivek Kumar Jain, N. Lakshmi, Rakesh Jain, Vishal Jain, Aarti R. Chandra, K. Venugopalan, J. Mater. Sci. 52 (11) (2017) 6800–6811.
- [10] P.V. Sreenivasa Reddy, V. Kanchana, G. Vaitheeswaran, David J. Singh, J. Phys. Condens. Matter 28 (2016) 115703.
- [11] J.H. Wernick, G.W. Hull, T.H. Geballe, J.E. Bernardini, J.V. Waszczak, Mater. Lett. 2 (1983) 90–92.
- [12] H.A. Kierstead, B.D. Dunlap, S.K. Malik, A.M. Umarji, G.K. Shenoy, Phys. Rev. B 32 (1985) 135.
- [13] Y.H. Qu, D.Y. Cong, X.M. Sun, Z.H. Nie, W.Y. Gui, R.G. Li, Y. Ren, Y.D. Wang, Acta Mater. 134 (2017) 236–248.
- [14] Hongliang Shi, Wenmei Ming, David S. Parker, Mao-Hua Du, David J. Singh, Phys. Rev. B 95 (2017) 195207.
- [15] C.W. Tseng, C.N. Kuo, H.W. Lee, K.F. Chen, R.C. Huang, C.M. Wei, Y.K. Kuo, C.S. Lue, Phys. Rev. B 96 (2017) 125106.
- [16] I. Knapp, B. Budinska, D. Milosavljevic, P. Heinrich, S. Khmelevskiy, R. Moser, R. Podloucky, P. Prenninger, E. Bauer, Phys. Rev. B 96 (2017) 045204.
- [17] Peng-Li Yan, Jian-Min Zhang, Ke-Wei Xu, Solid State Commun. 231–232 (2016) 64–67.
- [18] S. Aron-Dine, G.S. Pomrehn, A. Pribram-Jones, K.J. Laws, L. Bassman, Phys. Rev. B 95 (2017) 024108.
- [19] L. Van Hove, Phys. Rev. B 89 (1953) 11891193.
- [20] Y.M. Blanter, M.I. Kaganov, A.V. Pantsulaya, A.A. Varlamov, Phys. Rep. 245 (1994) 159257.
- [21] S.B. Dugdale, Phys. Scripta 91 (2016) 053009.

- [22] Y.O. Kvashnin, W. Sun, I. Di Marco, O. Eriksson, *Phys. Rev. B* 92 (2015) 134422.
- [23] P.V. Sreenivasa Reddy, V. Kanchana, G. Vaitheeswaran, Andrei V. Ruban, N.E. Christensen, *J. Phys. Condens. Matter* 29 (2017) 265801.
- [24] P.V. Sreenivasa Reddy, V. Kanchana, G. Vaitheeswaran, P. Modak, Ashok K. Verma, *J. Appl. Phys.* 119 (2016) 075901.
- [25] Hehe Zhang, Mingfang Qian, Xuexi Zhang, Sida Jiang, Longsha Wei, Dawei Xing, Jianfei Sun, Lin Geng, *Mater. Des.* 114 (2017) 1–9.
- [26] J.W. Christian, *The Theory of Transformations in Metals and Alloys* Part I, Pergamon Press, Amsterdam, 2002.
- [27] P. Blaha, K. Schwarz, P. Sorantin, S.B. Tricky, *Comput. Phys. Commun.* 59 (1990) 399–415.
- [28] J.P. Perdew, K. Burke, M. Ernzerhof, *Phys. Rev. Lett.* 77 (1996) 3865–3868.
- [29] H.J. Monkhorst, J.D. Pack, *Phys. Rev. B* 13 (1976) 5188.
- [30] P. Blochl, O. Jepsen, O. Andersen, *Phys. Rev. B* 49 (1994) 16223.
- [31] F. Birch, *Phys. Rev.* 71 (1947) 809.
- [32] Ali H. Reshak, Morteza Jamal, *J. Alloy. Comp.* 543 (2012) 147–151.
- [33] M. Born, *J. Chem. Phys.* 7 (1939) 591.
- [34] R. Hill, *Proc. Phys. Soc.* 65 (1952) 349.
- [35] V. Kanchana, *Eur. Phys. Lett.* 87 (2009) 26006.
- [36] V. Kanchana, G. Vaitheeswaran, Yanming Ma, Yu Xie, A. Svane, O. Eriksson, *Phys. Rev. B* 80 (2009) 125108.
- [37] V. Kanchana, G. Vaitheeswaran, A. Svane, *J. Alloy. Comp.* 455 (2008) 480.
- [38] J.J. Wortman, R.A. Evans, *J. Appl. Phys.* 36 (1965) 153.
- [39] S.F. Pugh, *Phil. Mag.* 45 (1954) p.823.
- [40] Z.G. Xu, J.W. Brill, *Phys. Rev. B* 43 (1991) 11037.